

See discussions, stats, and author profiles for this publication at: <https://www.researchgate.net/publication/233972849>

Photonic Modulation of Electron Transfer with Switchable Phase Inversion

ARTICLE *in* THE JOURNAL OF PHYSICAL CHEMISTRY A · DECEMBER 2012

Impact Factor: 2.69 · DOI: 10.1021/jp3106887 · Source: PubMed

CITATIONS

14

READS

18

6 AUTHORS, INCLUDING:



Gerdenis Kodis

Arizona State University

75 PUBLICATIONS 2,399 CITATIONS

SEE PROFILE



Thomas A Moore

Arizona State University

331 PUBLICATIONS 16,768 CITATIONS

SEE PROFILE

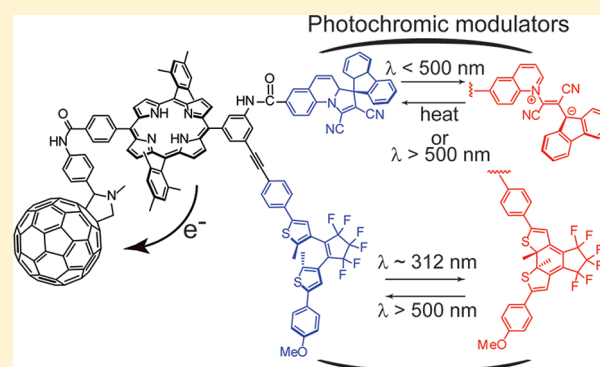
Photonic Modulation of Electron Transfer with Switchable Phase Inversion

Julien Frey, Gerdenis Kodis, Stephen D. Straight, Thomas A. Moore,* Ana L. Moore,* and Devens Gust*

Department of Chemistry and Biochemistry, Arizona State University, Tempe, Arizona 85287, United States

S Supporting Information

ABSTRACT: Photochromes may be reversibly photoisomerized between two metastable states and their properties can influence, and be influenced by, other chromophores in the same molecule through energy or electron transfer. In the photochemically active molecular tetrad described here, a porphyrin has been covalently linked to a fullerene electron acceptor, a quinoline-derived dihydroindolizine photochrome, and a dithienylethene photochrome. The porphyrin first excited singlet state undergoes photoinduced electron transfer to the fullerene to generate a charge-separated state. The quantum yield of charge separation is modulated by the two photochromes: one isomer of each quenches the porphyrin excited state, reducing the quantum yield of electron transfer to near zero. Interestingly, when the molecule is illuminated with white light, the quantum yield *decreases* as the white light intensity is increased, generating an out-of-phase response of the quantum yield to white light. However, when the same experiment is performed in the presence of additional, steady-state UV illumination, a phase inversion occurs. The quantum yield of electron transfer now *increases* with increasing white light intensity. Such effects illustrate emergent complexity in a relatively simple system and could find applications in molecular logic, photochemical labeling and drug delivery, and photoprotection for artificial photosynthetic molecules. The photochemistry leading to this behavior is discussed.



INTRODUCTION

When two chromophores are present in the same molecule, they can interact with one another. If the interaction is by photoinduced electron transfer, the resulting donor–acceptor systems are of interest as artificial photosynthetic reaction centers, molecular electronic elements, and related devices. When the interaction is by energy transfer, the systems can mimic photosynthetic antenna and photoprotective mechanisms, play roles in biomedical science and treatment, etc. When one of the chromophores is a photochrome, the additional element of photoisomerism comes into play. Photochromic molecules are isomerized between two metastable forms by light, or light and heat. The isomers have different absorption spectra and other photochemical properties and thus can interact differently with nearby chromophores. A photochrome is a photochemical analogue of a bistable electrical switch, or transistor, and molecules containing photochromes may function as Boolean binary logic devices of many kinds.^{1–8}

However, an ensemble of photochromic molecules, such as a solution, forms a photostationary state upon illumination in which the ratio of the two isomers is essentially infinitely variable. This property allows the design of analogue molecular devices. For example, we recently reported a molecular photonic analogue of a triode tube, or transistor amplifier, in which irradiation of a solution of the molecules with long-

wavelength light of modulated intensity in turn modulated the intensity of shorter-wavelength fluorescence induced by steady-state illumination at a different wavelength.⁹ In another example of this effect, we reported an artificial photosynthetic construct that functionally mimics a photoregulatory mechanism found in cyanobacteria.¹⁰ The molecule included a porphyrin–fullerene artificial reaction center that demonstrates photoinduced electron transfer, two antenna chromophores, and a photochrome. The quantum yield of photoinduced electron transfer was demonstrated to be inversely related to the intensity of white light excitation. This general behavior is also found in cyanobacteria, where the quantum yield of photosynthetic charge separation decreases as the light intensity increases.

Here, we report the synthesis and properties of molecular tetrad **1** (Figure 1), which consists of a porphyrin (P)–fullerene (C₆₀) charge-separation unit linked to both a quinoline-derived dihydroindolizine photochrome (DHI) and a dithienylethene photochrome (DTE). Excitation of the porphyrin moiety initiates photoinduced electron transfer to the fullerene to form a P^{•+}–C₆₀^{•–} charge-separated state. Each photochrome can be independently isomerized between an isomer that has no effect upon P–C₆₀ photoinduced electron

Received: October 29, 2012

Revised: December 10, 2012

Published: December 21, 2012

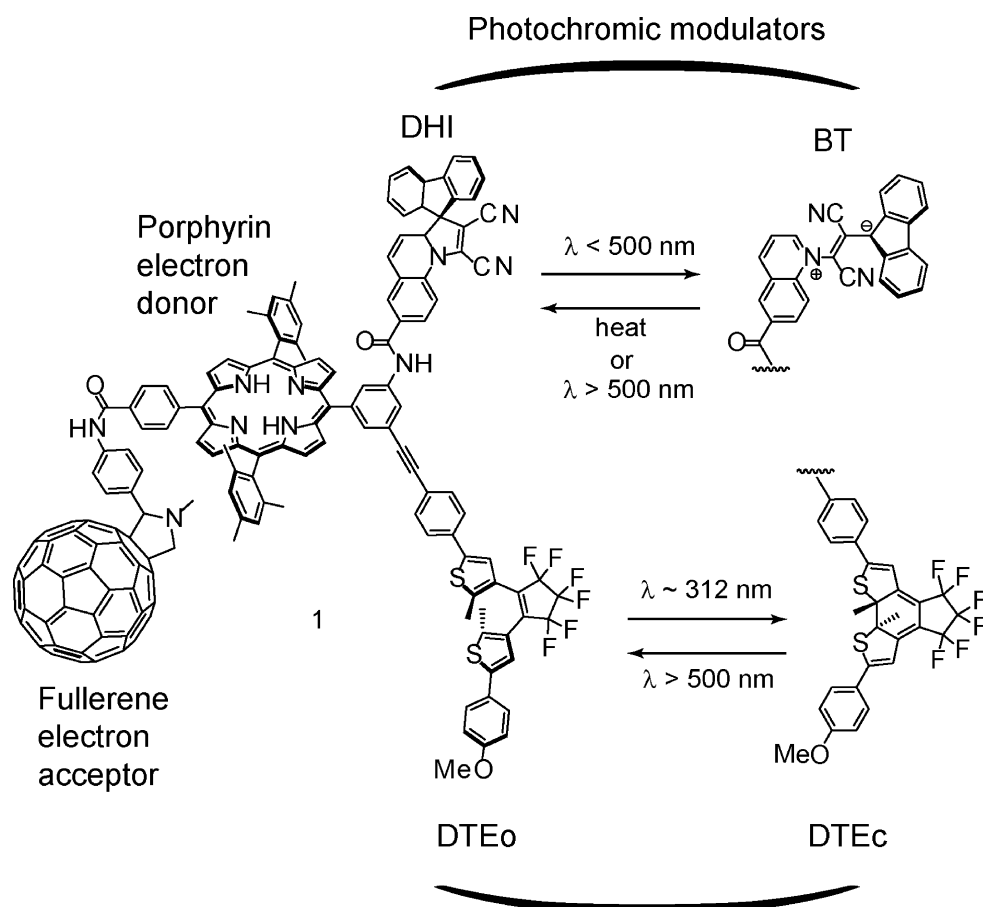


Figure 1. Tetrad **1** and isomerization pathways. In the structure at left, both photochromes are shown in their short-wavelength-absorbing forms (DHI and DTEo). At right are shown the photochrome moieties in their long-wavelength-absorbing forms (BT and DTEc). The arrows indicate conditions for isomerization of each photochrome.

transfer, and a form that strongly quenches electron transfer. As shown in Figure 2, this molecule shows unusual photochemistry. In a series of experiments (abscissa in the figure), a solution of the molecule in 2-methyltetrahydrofuran was irradiated with white light ($\lambda > 360 \text{ nm}$) until a photostationary distribution was reached, and the quantum yield of photoinduced electron transfer in the P–C₆₀ unit was determined. It was found that modulation of the white light intensity in turn modulates the yield of charge separation in an inverse fashion. That is, the waveform exhibited by the charge separation yield is 180° out-of-phase with the white light modulation: the more intense the white light, the *lower* the quantum yield of electron transfer. Next, a constant intensity of UV light ($\sim 312 \text{ nm}$) was applied, and the white light modulation experiment was repeated. The yield of photoinduced electron transfer was again found to be modulated according to the waveform of the white light, but now the waveform was in-phase with the white light: the more intense the white light, the *higher* the quantum yield of electron transfer. If the UV light was turned off, the tetrad returned to its previous behavior mode. Thus, the molecule is analogous to an electronic signal transducer with phase inversion capability. The remainder of this report explains the photochemical bases for this intriguing phenomenon.

RESULTS AND DISCUSSION

Synthesis. Tetrad **1** was prepared by the synthesis of a suitable substituted porphyrin, the attachment of the DTE photochrome by copper-free Sonogashira coupling, the linkage of the DHI photochrome to the porphyrin via amide bond formation, and finally the coupling to the fullerene via a second amide function. The necessary DHI¹⁰ and DTE¹¹ photochromes as well as the fullerene derivative¹² were prepared according to previously reported procedures. The model compounds **2**, **3**, and **4** (Figure 3) required for the spectroscopic study were prepared following similar schemes. Experimental procedures and characterization of the compounds are available in the Supporting Information.

Photochemistry of the Component Chromophores.

Understanding the behavior of the tetrad requires knowledge of the photochemical behavior of the various components. Previous studies¹³ of porphyrin–fullerene dyad **5** (Figure 4), which is closely related to the porphyrin–fullerene component of **1**, in 2-methyltetrahydrofuran have revealed that excitation of the porphyrin to give the first excited singlet state is followed by photoinduced electron transfer with a time constant of 2.0 ns to yield the P^{•+}–C₆₀^{•–} charge-separated state with a quantum yield of 80%. This charge-separated state lies 1.59 eV above the ground state and thus preserves a significant fraction of the porphyrin excitation energy (1.9 eV) as electrochemical potential. The P^{•+}–C₆₀^{•–} species decays to the ground state in 4.0 ns by charge recombination.

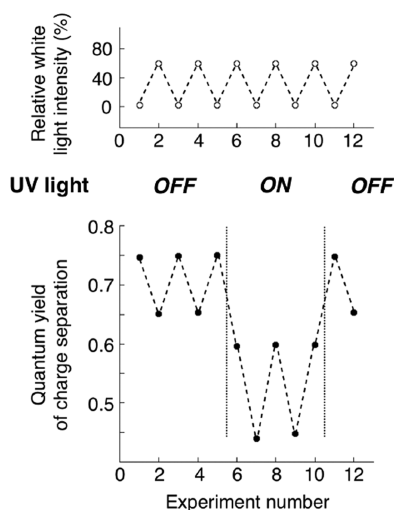


Figure 2. Phase inversion in modulation of photoinduced charge separation quantum yield in **1**. The upper part of the figure shows the relative intensity of white light used to irradiate a solution of **1** in 2-methyltetrahydrofuran in 12 experiments. The lower part of the figure shows the corresponding quantum yield of $P^{*+}-C_{60}^{*-}$ for each experiment after reaching the photochrome photostationary distribution. The vertical dotted lines divide experiments with no steady-state UV irradiation from those with UV irradiation. Note that the waveform of the quantum yield plot is 180° out-of-phase with that of the white light plot in the absence of UV irradiation, but in-phase when UV irradiation is present.

The structure of model dihydroindolizine (**6**) in its UV-absorbing form is shown in Figure 4, and its absorption spectra appear in Figure 5a.¹⁰ The spiro form, DHI, has an absorption band maximum at 395 nm in 2-methyltetrahydrofuran. Irradiation into this band causes photoisomerization to yield a photostationary distribution consisting mainly of the zwitterionic betaine form BT, which has maxima at 685 and 485 nm. A small amount of the DHI form is still present at the steady state. In the dark, BT thermally reverts fully to DHI with a time constant of 39 s at 25 °C. The BT isomer photochemically isomerizes to DHI as well, but the thermal process is faster at ambient temperatures and moderate white light intensities such as those used for the majority of the studies reported here. It will be noted that both the DHI and BT isomers absorb strongly at ~ 312 nm, with the extinction coefficient of BT somewhat larger than that of DHI. If the sample is driven mainly to BT by irradiation around 400 nm and then subjected to 312 nm irradiation, the photostationary distribution changes to feature more of the DHI isomer. Time-resolved measurements showed that the excited singlet state of the BT form of **6** is very short-lived, decaying with a time constant of 0.9 ps.¹⁰

Figure 5b shows the absorption spectra of model DTE **7** (Figure 4) in the open and closed forms.¹¹ The open form, DTEo, was generated by irradiation of a 2-methyltetrahydrofuran solution with 600 nm light. It features bands in the UV at 283 and 305 nm, with no significant absorption in the visible. The excited singlet state lifetime of DTEo in **7** is 25 ps.¹¹ Irradiation of the DTEo form at 360 nm converts it to a photostationary distribution consisting mainly of the DTEc form, which has absorption maxima at 320, 370 (sh), and 600 nm. Time-resolved emission studies of such a solution yielded a lifetime of 1.2 ps for ¹DTEc. The molecule is thermally stable in

either form, and therefore, interconversion between them requires light of the appropriate wavelengths.

Photochemistry of Triads and Tetrad. Tetrad **1** can exist in four isomeric forms (see Figure 1). In one thermally stable form, DHI-DTEo-P-C₆₀, the two photochromes are in the short-wavelength absorbing forms. Irradiation of a solution of this isomer in 2-methyltetrahydrofuran solution with white light ($\lambda > 360$ nm, ~ 600 mW/cm²) converts it to a solution consisting mainly of BT-DTEo-P-C₆₀ in which the dihydroindolizine is present as the betaine. This isomer thermally reverts to DHI-DTEo-P-C₆₀ with a time constant of 37 s at 25 °C. This time constant is essentially the same as that observed for model photochrome **6**. Alternatively, if the sample of DHI-DTEo-P-C₆₀ is exposed to UV light (~ 366 nm, 1.5 mW/cm², 3 min), it is converted to BT-DTEc-P-C₆₀ in which both photochromes are in the long wavelength absorbing forms. Finally, if BT-DTEc-P-C₆₀ is allowed to stand at ambient temperatures for a few minutes, the BT reverts thermally to DHI as discussed above, yielding DHI-DTEc-P-C₆₀. Irradiating this material with white light and then allowing it to thermally revert regenerates DHI-DTEo-P-C₆₀.

Each isomer of **1** has a unique absorption spectrum, as shown in Figure 6. In DHI-DTEo-P-C₆₀, the absorption at wavelengths longer than 450 nm is due mainly to the porphyrin Q-bands at 647, 591, 550, 516, and 482 (sh) nm. The porphyrin Soret band appears at 422 nm. These absorptions are typical of porphyrins of this type and are not perturbed by the attached photochromes or fullerene. The fullerene moiety has a very weak, nearly featureless absorption in the visible out to 705 nm that is not apparent in Figure 6. The DHI absorption at 395 nm (see Figure 5a) is present but mainly obscured by the much stronger Soret band. The DTEo bands at 283 and 305 nm (Figure 5) are also still present, but in addition the porphyrin, fullerene and DHI moieties have some absorption in this region. The BT-DTEo-P-C₆₀ isomer shows the same porphyrin, fullerene, and DTEo absorptions but also has relatively weak, broad absorption in the 450–750 nm region that is characteristic of BT (Figure 5a). Only subtle changes are seen in the UV region, as the disappearance of the 395 nm band of DHI is obscured by the porphyrin Soret. In BT-DTEc-P-C₆₀, strong, broad absorption is seen in the ca. 450–750 nm region. This arises mainly from DTEc, although there is also a small contribution from BT. In the UV region, there is an increase in absorption in the 340–400 nm region and a decrease in the 290–340 nm region that arise from the conversion of DTEo to DTEc. Upon thermal isomerization of this isomer to DHI-DTEc-P-C₆₀, there is little apparent change in the UV region and small absorbance decreases in the 450–800 nm region due to loss of the BT chromophore. Thus, the absorption spectra indicate that linkage of the four different chromophores to form **1** has little effect on the ground state absorption spectra of the individual chromophores. There are no strong interchromophore interactions that perturb absorption.

When the fluorescence spectra of the isomers are examined, strong differences are noted. The DHI-DTEo-P-C₆₀ shows typical porphyrin fluorescence at ca. 650 and 720 nm when excited at wavelengths absorbed mainly by the porphyrin moiety, although the intensity is reduced relative to that from porphyrin model compounds due to photoinduced electron transfer to the fullerene (see below). No significant emission from the other chromophores is observed. However, in BT-DTEo-P-C₆₀, DHI-DTEc-P-C₆₀, and BT-DTEc-P-C₆₀,

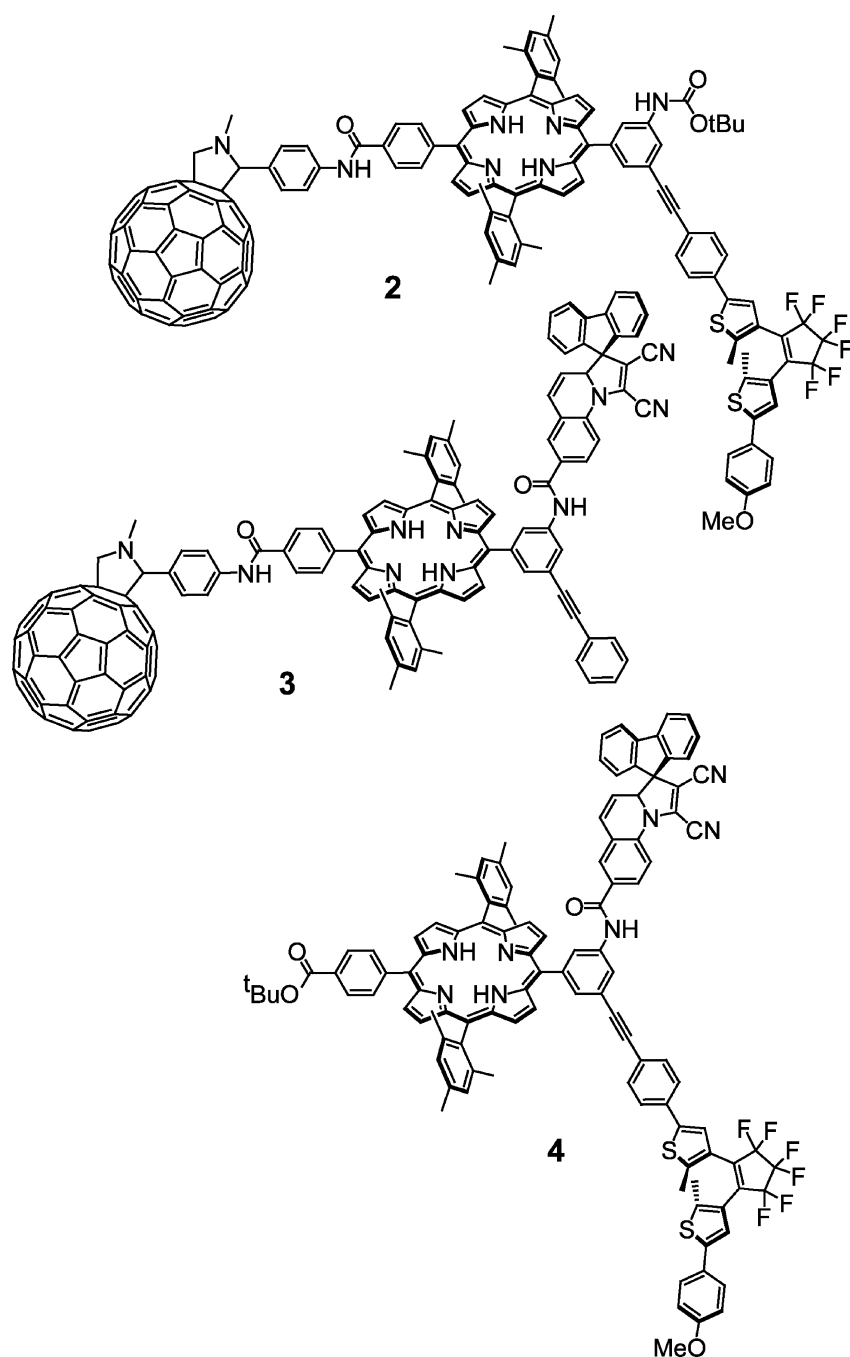


Figure 3. Structures of model DTE-P-C₆₀ **2**, model DHI-P-C₆₀ **3**, and model DHI-DTE-P **4**. The photochromes may also exist in the DTEc and BT forms, as in Figure 1.

the porphyrin emission is strongly quenched. Thus, both BT and DTEc quench the porphyrin first excited singlet state, and DHI-DTEo-P-C₆₀ is the only form of **1** that features significant fluorescence emission. The quenching cannot readily be investigated quantitatively using steady-state spectroscopy because a small amount of DHI-DTEo-P-C₆₀ can dominate the observed fluorescence, and the photostationary distributions obtainable are not completely pure isomeric states (except for DHI-DTEo-P-C₆₀). Time-resolved studies of **1** and model dyads **2–4** were performed to clarify the situation.

A deoxygenated 2-methyltetrahydrofuran solution of compound **4** was irradiated with UV light at ~366 nm as discussed above to convert most of the sample to the BT-DTEc-P form.

The solution was then excited with a 100 fs laser pulse at 390 nm. The porphyrin fluorescence decay over the 600–800 nm region was analyzed to generate kinetic fits ($\chi^2 = 1.19$) showing two exponential components of 12 ps (91%) and 11.0 ns (9%). The 11.0 ns component is assigned to the unquenched porphyrin of residual DHI-DTEo-P and represents decay of the porphyrin first excited singlet state by the usual photo-physical processes of internal conversion, intersystem crossing, and fluorescence.¹³ Thus, the photochromes in the DHI and DTEo forms have no influence on the porphyrin excited state lifetime. The 12 ps component is assigned to BT-DTEc-P, whose porphyrin first excited singlet state is strongly quenched

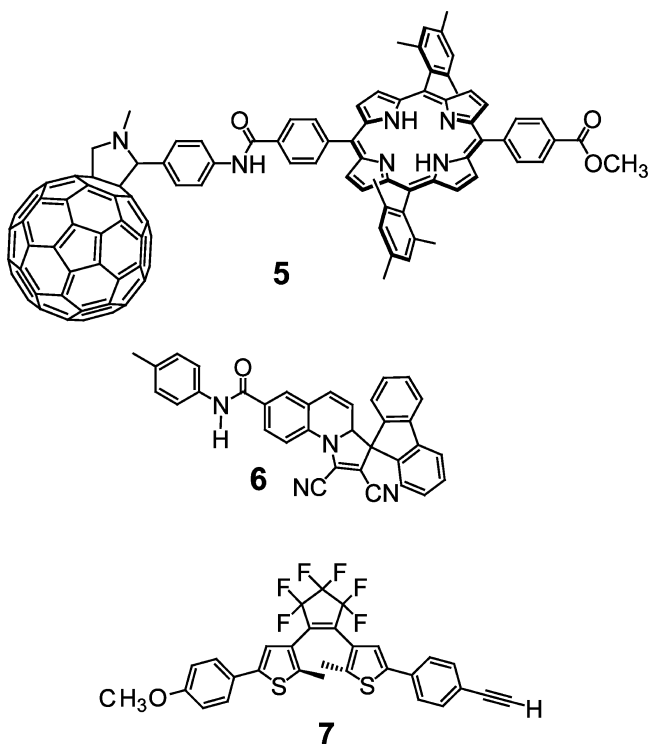


Figure 4. Structures of model P-C₆₀ **5**, DHI **6**, and DTE **7**. The two photochromes are shown in their short-wavelength-absorbing forms.

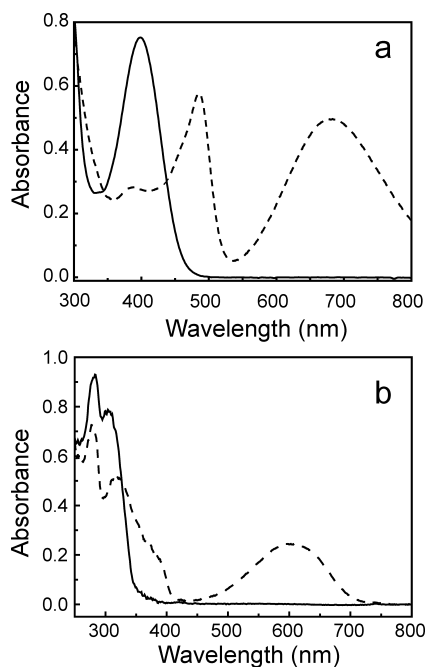


Figure 5. (a) Absorption spectra in 2-methyltetrahydrofuran of model compound **6** in its DHI (solid line) and BT (dashed line) forms. (b) Absorption spectra in 2-methyltetrahydrofuran of DTE model compound **7** in its DTEo (solid line) and DTEc (dashed line) forms.

by BT and DTEc, as suggested by the steady-state fluorescence studies of **1**.

Similar experiments were carried out on triad **3** in which DHI is the only photochrome. The deoxygenated solution was irradiated with UV light (~ 366 nm) in order to convert a portion of the sample to BT-P-C₆₀. The porphyrin emission

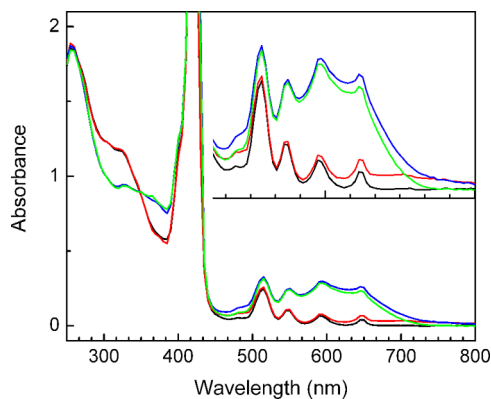


Figure 6. Absorption spectra of the isomers of **1** in 2-methyltetrahydrofuran. The spectra are from solutions highly enriched in the indicated isomers: DHI-DTEo-P-C₆₀ (black), BT-DTEo-P-C₆₀ (red), DHI-DTEc-P-C₆₀ (green), and BT-DTEc-P-C₆₀ (blue). The inset is a vertical expansion of the 450–800 nm region.

was fitted as described above ($\chi^2 = 1.17$) with two exponential components of 11 ps (25%) and 1.9 ns (75%). The 11 ps component corresponds to porphyrin emission from BT-P-C₆₀ and the 1.9 ns component to porphyrin emission from DHI-P-C₆₀. Clearly, in both compounds, the porphyrin first excited singlet state is quenched from its usual lifetime of 11 ns. In DHI-P-C₆₀ the quenching is due only to photoinduced electron transfer to the fullerene to give DHI-P^{•+}-C₆₀^{•-}. The rate constant for photoinduced electron transfer k_{ET} may be calculated from eq 1, where τ_s is the measured lifetime of the porphyrin first excited singlet state (1.9 ns), and k_D is the lifetime of the first excited singlet state in the absence of electron transfer. A value of 9.1×10^7 s⁻¹ for k_D may be estimated from the 11 ns lifetime measured for DHI-DTEo-P, giving $k_{ET} = 4.4 \times 10^8$ s⁻¹. The corresponding time constant for photoinduced electron transfer of 2.3 ns is very similar to that discussed above for model P-C₆₀ compound **5**.¹³ The corresponding quantum yield for photoinduced electron transfer, Φ_{ET} , is 0.83.

$$k_{ET} = \frac{1}{\tau_s} - k_D \quad (1)$$

Turning now to the results for BT-P-C₆₀, the decay of the porphyrin first excited singlet state is described by eq 2, where τ_s equals 11 ps, and k_{BT} is the rate constant for quenching of the porphyrin first excited singlet state by energy transfer to BT and equals 9.0×10^{10} s⁻¹. The quantum yield of energy transfer is 0.99.

$$k_{BT} = \frac{1}{\tau_s} - k_D - k_{ET} \quad (2)$$

Time-resolved emission studies of a solution of model compound **2** containing both DTEc-P-C₆₀ and DTEo-P-C₆₀ were performed as discussed above with excitation at 430 nm. These yielded a decay that was fitted ($\chi^2 = 1.19$) with two exponential components of 16 ps (37%) and 1.9 ns (63%). The percentages reflect the relative amounts of the two isomers present under the conditions of the experiment. The 1.9 ns component corresponds to DTEo-P-C₆₀. As was the case for DHI-P-C₆₀, the quenching of the porphyrin first excited singlet state from ca. 11 to 1.9 ns is due to photoinduced electron transfer to the fullerene, with $k_{ET} = 4.4 \times 10^8$ s⁻¹. The 16 ps time constant arises from DTEc-P-C₆₀, and the

additional quenching of the porphyrin first excited singlet state is ascribed to singlet–singlet energy transfer to DTEc. Using an equation analogous to eq 2, the rate constant for energy transfer, k_{DTEc} is found to be $6.2 \times 10^{10} \text{ s}^{-1}$, and the quantum yield of energy transfer is 0.99.

Time-resolved emission studies of **1** enriched in the BT–DTEc–P–C₆₀ isomer were performed in 2-methyltetrahydrofuran as described above, with excitation at 390 nm. The decay curves throughout the porphyrin emission region were fitted ($\chi^2 = 1.19$) with two exponential components of 12 ps (70%) and 1.9 ns (30%). The 12 ps component is ascribed to the decay of BT–DTEc–¹P–C₆₀ by singlet energy transfer to BT and DTEc, as was observed for the model compounds discussed above. The 1.9 ns decay is due to some DHI–DTEo–P–C₆₀ in the solution. The similarity of the time constants measured for **1** and for the model compounds **2** and **3** shows that the rate constants for the various decay pathways of the porphyrin first excited singlet state of **1** in its various isomeric forms are similar to those found for the model compounds and listed above.

White Light Modulation Experiments. Figure 7 shows the results of 15 experiments in which a stirred 2-

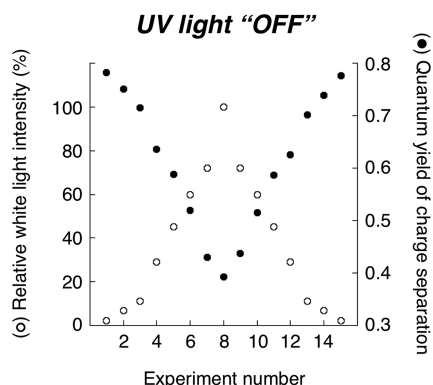


Figure 7. Effect of white light modulation on a solution of tetrad **1** in 2-methyltetrahydrofuran at 25 °C. The results of 15 experiments are shown. The stirred solution was irradiated with white light ($\lambda > 360 \text{ nm}$; 12 V, 150 W tungsten-halogen lamp with a 380 nm long-pass filter and different neutral density filters) at different relative intensities (hollow circles) until a steady-state distribution was reached, and the relative porphyrin fluorescence intensity at 720 nm ($\lambda_{\text{ex}} = 450 \text{ nm}$) was determined. This intensity was used to calculate the quantum yield of photoinduced electron transfer (solid circles) as explained in the text.

methyltetrahydrofuran solution of **1** was illuminated with white light ($\lambda > 360 \text{ nm}$) at various intensities (hollow circles) until a photostationary distribution was obtained (30 s); the porphyrin moiety was excited with a low-intensity beam at 450 nm, and the fluorescence intensity at 720 nm was recorded. This fluorescence intensity was used to determine the quantum yield of photoinduced electron transfer to give the $\text{P}^{\bullet+}\text{--C}_{60}^{\bullet-}$ charge-separated state based upon total light absorption by porphyrin chromophores in the solution (filled circles in Figure 7). This calculation was done by recognizing that of the four possible species in solution, DHI–DTEo–P–C₆₀, DHI–DTEc–P–C₆₀, BT–DTEo–P–C₆₀, and BT–DTEc–P–C₆₀, only DHI–DTEo–P–C₆₀ yields significant porphyrin fluorescence and photoinduced electron transfer, as the porphyrin excited states of the other three isomers are very strongly quenched by energy transfer processes. The quantum yield of electron transfer for DHI–DTEo–P–C₆₀ is 0.83, as discussed above. When the sample is illuminated with white light, photoisomerization occurs, and the mole fraction of DHI–DTEo–P–C₆₀ in the solution decreases; this leads to a decrease in the fluorescence intensity and a proportional decrease in quantum yield of electron transfer. Thus, the quantum yield of electron transfer by the solution may be determined from the fluorescence intensity relative to that from pure DHI–DTEo–P–C₆₀.

The behavior in Figure 7 may be discussed in terms of Figure 8, which recapitulates the four isomeric forms of **1** and the net results of irradiation of each form with UV or white light and of the influence of heat from the ambient environment. In Figure 7, it is seen that in experiments 1–8, as the white light intensity is gradually increased, there is a concomitant decrease in quantum yield of charge separation. This behavior may be rationalized based on the photophysical and photochemical results reported in the last sections. At the beginning of the series, all **1** is present as DHI–DTEo–P–C₆₀. White light of $>360\text{--}750 \text{ nm}$ excites DHI, BT, and DTEc, but not DTEo. Thus, white light irradiation converts the sample to a mixture of DHI–DTEo–P–C₆₀ and BT–DTEo–P–C₆₀. Although conversion of DHI to BT occurs photochemically, conversion of BT to DHI occurs mainly thermally at these light intensities. Thus, increasing the white light intensity increases the rate of conversion of DHI–DTEo–P–C₆₀ to BT–DTEo–P–C₆₀ but has relatively little effect on the rate of the reversion of BT–DTEo–P–C₆₀ to DHI–DTEo–P–C₆₀ and consequently decreases the concentration of DHI–DTEo–P–C₆₀ and the

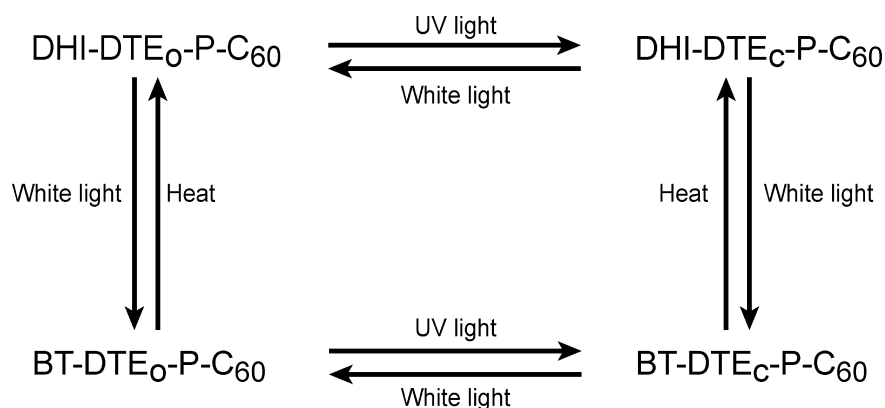


Figure 8. Isomeric forms and major interconversion pathways for tetrad **1**. Irradiation of any isomer with a particular wavelength distribution (UV, etc.) generates a photostationary distribution that is highly enriched in the indicated product isomers.

quantum yield of charge separation, based upon light absorbed by the porphyrin moieties. When the white light intensity is decreased, the rate of production of BT-DTEo-P-C₆₀ decreases, but the rate of thermal reversion does not, the mole fraction of DHI-DTEo-P-C₆₀ in the photostationary distribution increases, and the quantum yield increases (experiments 9–15 in Figure 7). This behavior leads to the inverse dependence of charge separation quantum yield upon white light intensity seen in experiments 1–5, 11, and 12 in Figure 2. In those experiments, the waveform of the quantum yield is 180° out-of-phase with the white light waveform.

Dual Light Experiments. Figure 9 shows the results of a series of experiments identical to those shown in Figure 7, with

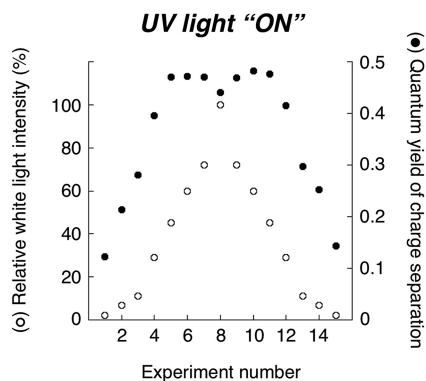


Figure 9. Results of a series of 15 experiments in which the sample of **1** in 2-methyltetrahydrofuran at 25 °C was irradiated with UV light (~312 nm) at 100% relative intensity and concurrently with white light ($\lambda > 360$ nm) of different intensities (hollow circles) until photostationary distributions were obtained. Then, the porphyrin moieties were excited at 450 nm and the relative fluorescence intensities measured. The quantum yields for charge separation (filled circles) were calculated from the fluorescence quenching as in Figure 7. The UV light intensity and the maximum white light intensity were the same as for the experiments shown in Figures 2 and 7. Irradiation time to reach a photostationary distribution was 8 min.

the exception that the sample was irradiated continuously with UV light (~312 nm and $\sim 95 \mu\text{W cm}^{-2}$) at a constant light flux during establishment of the photostationary distributions for each experiment. The behavior of **1** is very different under these conditions. In experiments 1–5 of Figure 9, the quantum yield of charge separation *increases* with increasing white light intensity, whereas it decreases with decreasing white light intensity in experiments 11–15. There is a pseudoplateau in quantum yield for experiments 5–11, and a slight decrease in experiment 8.

The response in Figure 9 can again be discussed in terms of Figure 8. As shown in Figure 5, all four forms of the photochromes absorb in the 312 nm spectral region. Thus, when the sample is irradiated at this wavelength with no white light irradiation (experiment 1 in Figure 9), the sample exists as a mixture of DHI-DTEo-P-C₆₀, DHI-DTEc-P-C₆₀, BT-DTEo-P-C₆₀, and BT-DTEc-P-C₆₀. Figure 5 shows that the photostationary distribution is heavily weighted in the quenching forms of the molecule, DHI-DTEc-P-C₆₀, BT-DTEo-P-C₆₀, and BT-DTEc-P-C₆₀. This accounts for the low quantum yield of charge separation. Increasing the white light intensity, as in experiments 2–5, photoisomerizes increasing amounts of DTEc to DTEo and therefore increases the mole fraction of BT-DTEo-P-C₆₀ and DHI-DTEo-P-

C₆₀. The DHI-DTEo-P-C₆₀ component is responsible for the increased quantum yield of charge separation. Thus, the yield of charge separation increases with increasing white light intensity. This in-phase dependence is also apparent in experiments 6–10 in Figure 2. In experiments 11–15 in Figure 9, decreasing the white light intensity decreases the quantum yield of charge separation, demonstrating that the phenomena being observed are indeed reversible and occurring under steady-state conditions at each experimental point.

It is interesting to note that at the highest white light intensities in Figure 9, the quantum yield approximately stabilizes at about 0.5. This occurs because at the higher white light intensities, conversion of DHI to BT begins to dominate over thermal reversion of BT to DHI. This effect is discussed in more detail later.

Figure 7 was obtained without UV irradiation and Figure 9 with the maximum level of UV irradiation employed in these studies. Figure 10 shows results where both UV and white light

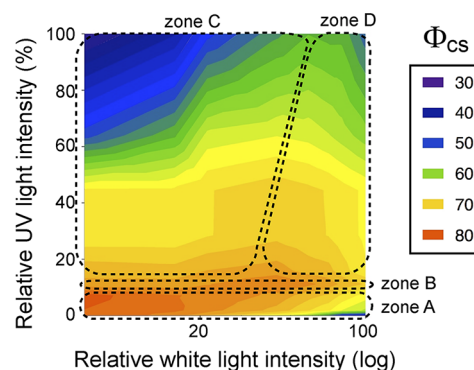


Figure 10. Quantum yield of charge separation (Φ_{CS}) from porphyrin excitation for a solution of tetrad **1** in 2-methyltetrahydrofuran at 25 °C as a function of the relative intensities of UV (~312 nm) and white ($\lambda > 360$ nm) light. The meaning of the various zones is discussed in the text.

intensities were altered. A sample of **1** in 2-methyltetrahydrofuran at 25 °C initially in the DHI-DTEo-P-C₆₀ form was simultaneously irradiated with both UV and visible light at different intensities until the photostationary distribution was reached, and the quantum yield for photoinduced electron transfer was determined as described above. The vertical axis reports the relative UV light intensity, the horizontal axis, the relative visible light intensity on a log scale, and the colors, the quantum yield of charge separation (Φ_{CS}). The data from which this plot was obtained are reported numerically in the Supporting Information.

In order to better understand Figure 10, it is useful to consider in more detail the composition of a solution of **1** under various combinations of excitation light. At any time, the total tetrad composition of the solution is described by eq 3, where $\chi_{\text{DHI-DTEo}}$ represents the mole fraction of DHI-DTEo-P-C₆₀, etc. Under illumination, the χ values will be those of the appropriate photostationary distribution, where the rate of formation of each isomer equals its rate of removal by conversion to other isomers. The rates of the photoisomerization processes depend in turn on the light intensity at each wavelength, the extinction coefficient of each chromophore at each wavelength, and the quantum yield of photoisomerization of each chromophore. The photostationary distribution also depends upon the temperature and the activation energy for

thermal isomerization of BT to DHI. Calculation of the exact distribution of isomers would be difficult, as some of the parameters are unknown, and because the sample was excited with broadband light covering a whole range of wavelengths rather than monochromatic light. However, the photochemistry of **1** discussed above as understood from the study of the various model compounds does allow a qualitative explanation for the behavior observed in Figure 10.

$$\chi_{\text{DHI-DTEo}} + \chi_{\text{BT-DTEo}} + \chi_{\text{DHI-DTEc}} + \chi_{\text{BT-DTEc}} = 1 \quad (3)$$

In the first place, the time-resolved spectroscopic results for compounds **2**, **3**, **4**, and **5** show that BT and DTEc quench the porphyrin first excited singlet state with quantum yields of essentially unity. Thus, the only isomer of **1** that demonstrates significant charge separation and fluorescence is DHI-DTEo-P-C₆₀. The Φ_{CS} data in Figure 10 therefore essentially reflect the fractional population of this isomer.

Before any irradiation of **1** in Figure 10, the sample was completely in the DHI-DTEo-P-C₆₀ form ($\chi_{\text{DHI-DTEo}} = 1$), and the quantum yield of charge separation was maximal (83%, lower left-hand corner of the plot). The white light used in these experiments ($\lambda > 360$ nm) is absorbed only by DHI, BT, and DTEc; DTEo is not affected. Thus, in the area roughly delineated by zone A of Figure 10, where there is little or no UV irradiation, the photostationary distribution consists essentially entirely of DHI-DTEo-P-C₆₀ and BT-DTEo-P-C₆₀ ($\chi_{\text{DHI-DTEo}} + \chi_{\text{BT-DTEo}} = 1$). The only processes contributing significantly to the photostationary distribution are photoisomerization of DHI to BT by light in the ca. 360–440 nm region (Figure 5a) and thermal conversion of BT to DHI. As noted above, photoisomerization of BT to DHI also occurs, but the thermal process is more efficient at low light levels at 25 °C. Increasing white light intensity increases $\chi_{\text{BT-DTEo}}$, the fraction of the quenched isomer, and this leads to the behavior observed in zone A, Figure 7, and the out-of-phase parts of Figure 2, where white light irradiation decreases Φ_{CS} .

Zone C in Figure 10 is the region where Φ_{CS} is in phase with the white light intensity, increasing as the white light intensity increases. In this region, the UV light is intense enough to drive a significant amount of DTEo into the quenching, DTEc form. Thus, $\chi_{\text{DHI-DTEc}}$ and $\chi_{\text{BT-DTEc}}$ increase at the expense of the other two isomers as the UV light intensity increases. At any given UV light intensity, increasing the intensity of white light in Zone C increases the rate of conversion of DTEc back to DTEo, and thus increases $\chi_{\text{DHI-DTEo}}$ and $\chi_{\text{BT-DTEo}}$. It also increases the rate of conversion of DHI to BT, as discussed above, but the rate of increase of $\chi_{\text{BT-DTEo}}$ with increasing white light is slower than that of $\chi_{\text{DHI-DTEo}}$ because thermal reversion of BT to DHI is still significant and drains population out of $\chi_{\text{BT-DTEo}}$ but not $\chi_{\text{DHI-DTEo}}$. The net result is that, in zone C, increasing white light intensity increases Φ_{CS} . In addition, the extinction coefficient of DTEc is high throughout much of the spectral region illuminated with white light (Figure 6), and this favors a rapid increase in the rate of conversion of DTEc to DTEo. These effects are also seen in Figure 9, experiments 2–4 and 11–15.

Zone B in Figure 10, where the UV intensity is about 10% of the maximum, represents a region in which UV irradiation has produced a mixture of all four isomers in solution. Increasing white light irradiation tends to increase both $\chi_{\text{DHI-DTEo}}$ and $\chi_{\text{BT-DTEo}}$ due to photoisomerization of DTEc, as in zone C, but this is balanced by increased conversion of DHI-DTEo-P-C₆₀

to BT-DTEo-P-C₆₀ as in zone A, and the net result is essentially no change in $\chi_{\text{DHI-DTEo}}$ and consequently in Φ_{CS} .

Finally, in zone D of Figure 10, it is seen that at any UV light intensity, further increasing the white light intensity somewhat decreases Φ_{CS} . Thus, at a given UV intensity, the quantum yield goes through a maximum, increasing with white light intensity throughout zone C and then decreasing with increasing white light intensity in zone D. The position of maximum Φ_{CS} shifts to higher white light intensities as the UV intensity is increased. For a given UV intensity, at the maximum Φ_{CS} , the $\chi_{\text{DHI-DTEo}}$ is maximized. When the white light intensity is increased beyond this maximum in Φ_{CS} , the rate of conversion of DHI to BT with increasing white light intensity increases, leading to an increase in $\chi_{\text{BT-DTEo}}$ at the expense of $\chi_{\text{DHI-DTEo}}$ and consequently a decrease in Φ_{CS} . This occurs because, at these high white light intensities, thermal conversion of BT to DHI (whose rate constant is independent of light intensity) is no longer very significant, relative to photochemical conversion of DHI to BT, and $\chi_{\text{BT-DTEo}}$ therefore increases more rapidly with white light intensity than does $\chi_{\text{DHI-DTEo}}$. This effect has also begun to appear in experiment 8, Figure 9.

Although the above effects qualitatively explain the behavior observed in Figures 2, 7, 9, and 10, there is another, less apparent facet to the photochemistry of this system. Experiments on model compound **3**, which lacks the DTE chromophore, show that, in the absence of UV irradiation, the maximum white light irradiation used in these experiments reduces Φ_{CS} from 82% to 40% (see Supporting Information). However, if steady-state UV irradiation anywhere from 9% to 100% of the maximum intensity used in these experiments is applied concurrently, the maximum white light irradiation only reduces Φ_{CS} to ~73%. The UV light greatly diminishes the effect of white light on the DHI/BT photostationary distribution in **3**, and presumably in **1** as well. Part of the reason for this is apparent from Figure 5, where it is seen that the extinction coefficient of BT is lower than that of DHI in the 360–440 nm region, but it is higher than or equal to that of DHI in the ≤ 312 nm region, where the UV light is applied. Thus, in the photostationary distribution under these conditions, photochemical production of BT is driven by white light irradiation, but reversion to DHI is driven both thermally and by UV irradiation, and the effectiveness of white light at increasing χ_{BT} is reduced.

CONCLUSIONS

The photochemistry of triad **1**, as detailed in Figure 10, is an excellent example of the complexity of behavior that emerges when two photochromes, each with its own unique properties, control the photochemistry of additional photoactive species in the molecule. The spectral differences among the chromophores of **1** shown in Figures 5 and 6 suggest that **1** would likely show additional nuances of behavior if the wavelengths used to activate the molecule were different than those used in this study. In addition to their fundamental interest, the kinds of effects observed in **1** could find applications in biomedical and other kinds of fluorescence labeling/imaging, photoprotection and photoregulation for artificial photosynthetic systems, photochemical drug release, and similar areas.

■ ASSOCIATED CONTENT

📄 Supporting Information

Experimental details of the synthesis and spectroscopic investigations. This material is available free of charge via the Internet at <http://pubs.acs.org>.

■ AUTHOR INFORMATION

Corresponding Author

*E-mail: gust@asu.edu (D.G.); tmoore@asu.edu (T.A.M.); amoore@asu.edu (A.L.M.).

Notes

The authors declare no competing financial interest.

■ ACKNOWLEDGMENTS

This work was supported by a grant from the U.S. National Science Foundation (CHE-0846943). A fellowship to J.F. was generously provided by the French Ministry of Foreign Affairs (Egide, Lavoisier Program).

■ REFERENCES

- (1) Andréasson, J.; Pischel, U.; Straight, S. D.; Moore, T. A.; Moore, A. L.; Gust, D. *J. Am. Chem. Soc.* **2011**, *133*, 11641–11648.
- (2) Gust, D.; Moore, T. A.; Moore, A. L. *Chem. Commun.* **2006**, 2006, 1169–1178.
- (3) Gust, D.; Andréasson, J.; Pischel, U.; Moore, T. A.; Moore, A. L. *Chem. Commun.* **2012**, *48*, 1947–1957.
- (4) Balzani, V.; Credi, A.; Venturi, M. *ChemPhysChem* **2003**, *3*, 49–59.
- (5) de Silva, A. P.; Uchiyama, S. *Nat. Nanotechnol.* **2007**, *2*, 399–410.
- (6) Szacilowski, K. *Chem. Rev.* **2008**, *108*, 3481–3548.
- (7) Raymo, F. M. *Adv. Mater.* **2002**, *14*, 401–414.
- (8) Andréasson, J.; Pischel, U. *Chem. Soc. Rev.* **2010**, *39*, 174–188.
- (9) Keirstead, A. E.; Bridgewater, J. W.; Terazono, Y.; Kodis, G.; Straight, S.; Liddell, P. A.; Moore, A. L.; Moore, T. A.; Gust, D. *J. Am. Chem. Soc.* **2010**, *132*, 6588–6595.
- (10) Straight, S. D.; Kodis, G.; Terazono, Y.; Hambourger, M.; Moore, T. A.; Moore, A. L.; Gust, D. *Nat. Nanotechnol.* **2008**, *3*, 280–283.
- (11) Liddell, P. A.; Kodis, G.; Moore, A. L.; Moore, T. A.; Gust, D. *J. Am. Chem. Soc.* **2002**, *124*, 7668–7669.
- (12) Terazono, Y.; Liddell, P. A.; Garg, V.; Kodis, G.; Brune, A.; Hambourger, M.; Moore, T. A.; Moore, A. L.; Gust, D. *J. Porphyrins Phthalocyanines* **2005**, *9*, 706–723.
- (13) Straight, S. D.; Andréasson, J.; Kodis, G.; Moore, A. L.; Moore, T. A.; Gust, D. *J. Am. Chem. Soc.* **2005**, *127*, 2717–2724.